Ripple Current Reduction of a Fuel Cell for a Single-Phase Isolated Converter Using a DC Active Filter With a Center Tap

Jun-ichi Itoh, *Member, IEEE*, and Fumihiro Hayashi

***Abstract*—A ripple current reduction method is proposed that does not require additional switching devices. A current ripple that has twice the frequency component of the power supply is generated in the dc part when a single-phase pulsewidth-modulated inverter is used for a grid connection. The current ripple causes shortening of the lifetime of electrolytic capacitors, batteries, and fuel cells. The proposed circuit realizes a dc active filter function without increasing the number of switching devices, because the energy buffer capacitor is connected to the center tap of the isolation transformer. In addition, the buffer capacitor voltage is controlled by the common-mode voltage of the inverter. The features of the proposed circuit, control strategy, and experimental results are described, including the result of ripple reduction, to approximately 20% that of the conventional circuit.**

***Index Terms*—Center tap, dc active filter, grid connection system, ripple current reduction, single-phase isolated converter.**

I. Introduction

RECENTLY, energy sources such as wind power systems, photovoltaic cells, and fuel cells have been extensively studied in response to global warming and environmental issues. The fuel cell is an important technology for new mobile applications and power grid distribution systems. For power distribution, fuel cell system requires a grid interconnection converter to supply power to the power grid. A grid interconnection converter using an isolation transformer is preferable for power grid distribution systems in terms of surge protection and noise reduction. In addition, size reduction and high efficiency are essential requirements [1]–[8].

One of the problems in the fuel cell system is that the lifetime is decreased by the ripple current. Therefore, in order to extend the lifetime, the fuel cell ripple current must be reduced in the grid interconnection converter [9], [10]. However, when a single-phase pulsewidth-modulated (PWM) inverter is used for grid connection system, the power ripple is twice the frequency of the power grid. Therefore, in conventional grid connection inverters, large electrolytic capacitors are connected in parallel to the fuel cell in order to reduce the current ripple. However, the use of large-sized electrolytic capacitors increases both the device volume and cost.

In order to reduce the current ripple in the fuel cell, some approaches use high-speed current control [11], [12]. This method incorporates a current-loop control within the existing dc–dc converter voltage loop. However, a large capacitor or reactor is required as an energy buffer. Other approaches have been proposed that do not require the use of large-sized electrolytic capacitors, e.g., an active filter is applied in the dc-link part [13]–[16]. The dc active filter consists of a small capacitor as an energy buffer, a reactor to reduce the switching ripple, and a dc chopper. The dc chopper injects the ripple current to avoid a power ripple. The capacitance can be lower, because the terminal voltage of the capacitor can be varied over a wide range. However, the number of the switching devices is increased, requiring a high-cost dc chopper and resulting in a large volume device. Other configurations of dc active filters have similar problems.

This paper proposes a new circuit topology including a dc active filter function without extra switching devices. The proposed circuit consists of an isolated dc/dc converter and interconnection inverter, and achieves the dc active filter function using the center tap of the isolation transformer. One feature of the proposed converter is that the primary-side inverter in the dc/dc converter is individually controlled by the common-mode voltage and the differential voltage. The ripple current is suppressed by the common-mode voltage control of the dc/dc converter, and the main power flow is controlled by the differential-mode voltage.

Conventional and proposed circuit topologies with the principle of current ripple suppression are first introduced. The control method of the proposed circuit is then described. In addition, the design of the energy buffer capacitor and transformer by which the maximum power ripple can be accepted is indicated. Furthermore, experimental results are presented in order to confirm the validity of the proposed circuit.

II. Proposed Circuit Configurations

Fig. 1 shows a conventional circuit that consists of a first-stage inverter for the medium frequency link, a transformer, a diode rectifier, and a grid interconnection inverter. When the interconnection current and power grid voltage are sinusoidal waveforms, the instantaneous power p of the grid interconnection is obtained by (1) at unity power factor

$$\begin{aligned} p &= \sqrt{2}I\,\sin(\omega t)\sqrt{2}V\,\sin(\omega t) \\ &= VI\{1-\cos(2\omega t)\} \end{aligned} \tag{1}$$

Manuscript received March 30, 2009; revised June 10, 2009. Current version published March 31, 2010. A part of this paper was presented at the IEEE Applied Power Electronics Conference 2009, Washington, DC. Recommended for publication by Associate Editor S. Choi.

J.-i. Itoh is with the Nagaoka University of Technology, Nagaoka, Niigata 940-2188, Japan (e-mail: itoh@vos.nagaokaut.ac.jp).

F. Hayashi was with the Nagaoka University of Technology, Nagaoka, Niigata 940-2188, Japan. He is now with Shikoku Electric Power Company, Inc., Kagawa 761-8573, Japan (e-mail: bunpaku@stn.nagaokaut.ac.jp).

Digital Object Identifier 10.1109/TPEL.2009.2029106

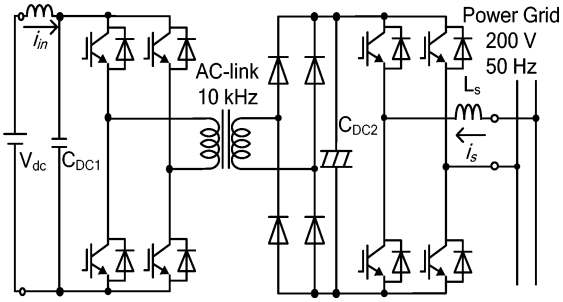

Fig. 1. Conventional circuit.

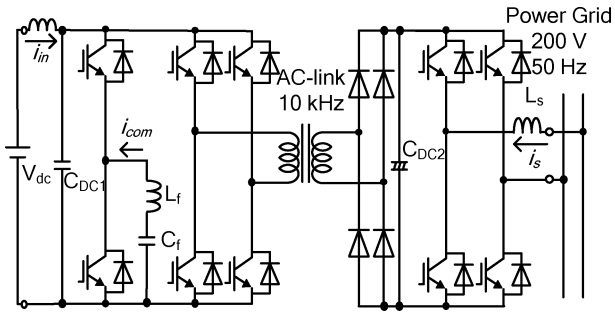

Fig. 2. Conventional circuit with dc active filter.

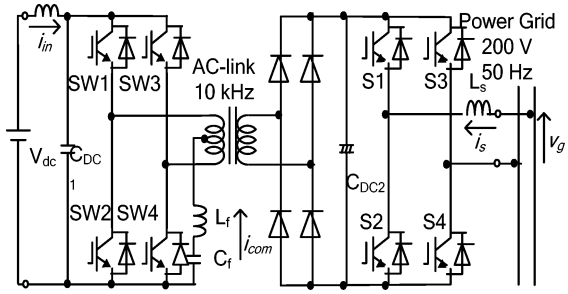

Fig. 3. Proposed circuit.

where I and V are the rms values of the interconnection current and the grid voltage, and ω is the grid angular frequency.

Thus, the instantaneous power has a ripple that is twice the frequency of the power grid frequency. To reduce the ripple power of a dc power source, such as a fuel cell, battery, or photovoltaic cell, large electrolytic capacitors $C_{\rm dc1}$ and $C_{\rm dc2}$ are used in the converter, as shown in Fig. 1. The use of large electrolytic capacitors precludes reduction in size and cost.

Fig. 2 shows the other conventional circuit using a dc active filter, which is constructed using a dc chopper and an energy buffer capacitor C_f. The capacitor C_f is used as an energy buffer to absorb the ripple power. The inductor L_f can suppress the switching current. The voltage of the capacitor C_f is controlled at twice the frequency of the power grid frequency. As a result, the ripple power does not appear in $V_{\rm dc}$, despite the use of small capacitors $C_{\rm dc1}$ and $C_{\rm dc2}$. However, the problem of this method is that the number of switching elements is increased.

Fig. 3 shows the proposed circuit, which combines the first-stage inverter and dc active filter functions. The energy buffer capacitor C_f is connected to the center tap of a medium-frequency transformer. The zero vector of the full-bridge first-stage inverter is used to control the center tap potential voltage. In addition, the leakage inductance of the transformer is used to suppress the switching current in addition to the boost reactor L_f. If the leakage inductance is large enough, then the boost reactor is not required.

TABLE I
COMPARISON OF THE NUMBER OF SWITCHING DEVICES AND THE CAPACITOR CAPACITY

	Device Number	DC Link Capacitor
Conventional Circuit	8	large
Conventional Circuit with DC Active Filter	10	small
Proposed Circuit	8	small

Table I provides a comparison of the number of switching devices and the capacitor capacity of a conventional circuit, a conventional circuit with a dc active filter, and the proposed circuit. The proposed circuit does not require additional switching devices or an inductor, in comparison to the conventional circuit with the dc active filter. It should be noted that the current ratings of the switching devices are larger than that of the conventional circuit, depending on the capacity of the energy buffer, because the dc active filter current flows in the first-stage inverter and the transformer.

III. Control Strategy

The first-stage inverter in the proposed circuit has two roles to perform: that of a dc/dc converter and that of a dc active filter. These roles are achieved by controlling the common-mode and differential-mode voltages in the first-stage inverter. This paper explains the principle of the proposed control method and the design method for the buffer capacitor and the transformer.

A. Switching Pattern Generation Method

Fig. 4 illustrates the two switching modes of the first-stage inverter in the proposed circuit. In the differential mode, the terminal voltage of the transformer is controlled, as shown in Fig. 4(a) and (b), and in the common mode, the center tap voltage is controlled, as shown in Fig. 4(c) and (d). When the differential mode is selected, the power transfers to the secondary side. It should be noted that the buffer current for the differential mode depends on the capacitor voltage. When the capacitor voltage is greater than half of the dc voltage, the buffer capacitor is charged. When the capacitor voltage is less than half of the dc voltage, the buffer capacitor is discharged. The inverter outputs the zero voltage vectors (00 and 11 are two) in common-mode operation. When the zero voltage vectors are selected, the line-to-line voltage of the transformer is zero. However, the center tap voltage is either $V_{\rm dc}$ or zero, depending on the zero vectors of Fig. 4(c) or (d), respectively. Thus, by controlling the ratio of the zero vectors, the buffer capacitor can be charged or discharged.

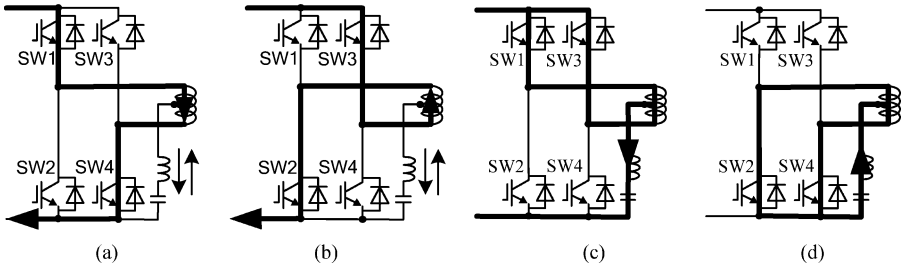

Fig. 4. Operation modes of the proposed circuit. (a) Differential mode 1. (b) Differential mode 2. (c) Common mode 1. (d) Common mode 2.

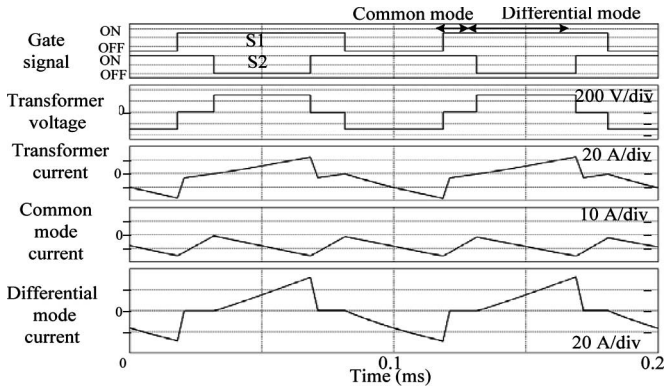

Fig. 5. Current and voltage waveforms for differential-mode and common-mode operations.

It should be noted that the output-switching pattern must include the zero vector period. Therefore, the voltage transfer ratio of the first-stage inverter is limited by the dc active filter control. As a result, the terminal voltage of the transformer is decreased.

Fig. 5 illustrates the operation waveforms with consideration of the transformer. The waveforms confirm that the transformer current consists of the common-mode current, which is the buffer current, and the differential-mode current. The common-mode current increases while S_1 and S_2 are turned on, and decreases during differential mode, because the capacitor voltage is greater than half of the dc voltage.

Fig. 6 shows a control block diagram of the proposed circuit. In order to suppress the ripple current of the fuel cell, all the current ripples are provided by the energy buffer capacitor. Therefore, the capacitor current command $i^*_{\rm com}$ is obtained by calculating the power ripple. The capacitor current $i_{\rm com}$ in the active buffer is controlled by a proportional–integral (PI) regulator to agree with the capacitor current command, and the dc active filter voltage command $v^*_{\rm com}$ is output by the PI regulator. In order to obtain the maximum terminal voltage of the transformer, the differential-mode voltage command $v^*_{\rm dif}$ is set to the maximum value. It should be noted that the maximum value of the voltage command is "1" when the peak value of the triangle carrier is "1."

The feature of the proposed circuit control is that the dc active filter voltage command $v^*_{\rm com}$ is added to the differential voltage command $v^*_{\rm dif}$ as the common-mode voltage. The output voltage commands v^*_1 and v^*_2 for each leg in the first-stage inverter are obtained by

$$\begin{cases} v^*_1 = \dfrac{1}{2}(v^*_{\rm com} + v^*_{\rm dif}) \\ v^*_2 = \dfrac{1}{2}(v^*_{\rm com} - v^*_{\rm dif}). \end{cases} \tag{2}$$

Grid interconnection control can be applied to the conventional control method, which uses an automatic current regulator (ACR) for the interconnection current command $I^*_{\rm grid}$. The interconnection current command is obtained by the synchronous signal to the grid voltage.

B. Design of the Buffer Capacitor for dc Active Filter Operation

The buffer capacitor is used as an energy storage element of the active filter. The capacitor C_f has to absorb the power ripple for a half cycle of the power grid. Thus, the required storage energy W_C is given by (3) from (1) and the capacitor energy W_f is obtained by (4)

$$W_C = \int_0^{\rm T/4} P_{\rm in}\ \cos 2\omega t dt = \frac{P_{\rm in}}{\omega} \tag{3}$$

$$W_f = \frac{1}{2} C_f \left(V^2_{f\max} - V^2_{f\min}\right) \tag{4}$$

where $P_{\rm in}$ is the input power, and $V_{f\max}$ and $V_{f\min}$ are the maximum and minimum voltages of C_f, respectively.

Therefore, the required capacitance C_f is given by (5) from (3) and (4) as

$$\begin{aligned} C_f &= \frac{2P_{\rm in}}{\omega((V_{c_{f0}} + \Delta V_{c_f}/2)^2 - (V_{c_{f0}} - \Delta V_{c_f}/2)^2)} \\ &= \frac{P_{\rm in}}{\omega V_{c_{f0}} \Delta V_{c_f}} \end{aligned} \tag{5}$$

where $V_{c_{f0}}$ and ΔV_{c_f} are the average voltage and the voltage variation of C_f, respectively.

Fig. 7 shows the relation between the capacitance and ΔV_{c_f} of the capacitor to compensate the power ripple at 1 kW and $V_{c_{f0}}$ of 150 V, according to (5). The capacitance can be significantly reduced by the capacitor voltage variation. It should be noted that the percentage impedance of the 1000 μF capacitor reciprocates with 3.18 p.u. based on 200 V, 50 Hz, and 1 kW.

The reactor L_f is set to decrease the switching ripple, i.e., L_f depends on the switching frequency of the first-stage inverter; the leakage inductance of the transformer is used as L_f.

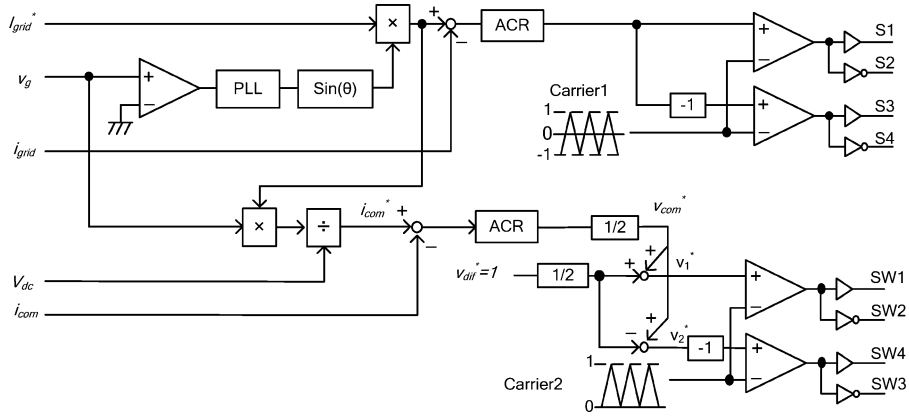

Fig. 6. Control block diagram of the proposed circuit.

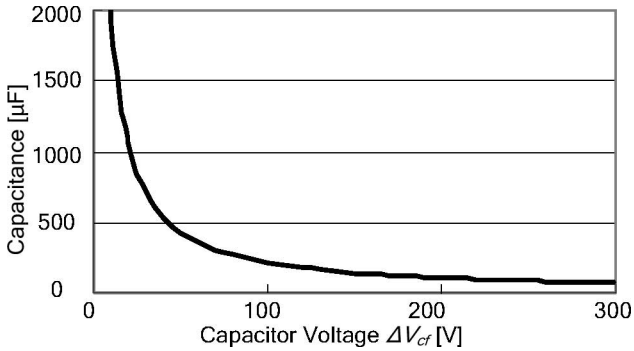

Fig. 7. Required capacitance for power ripple compensation. ($P_{\rm in} = 1$ kW, $V_{\rm dc} = 300$ V, $V_{cf0} = 150$ V, 1000 μF = 3.18 p.u.).

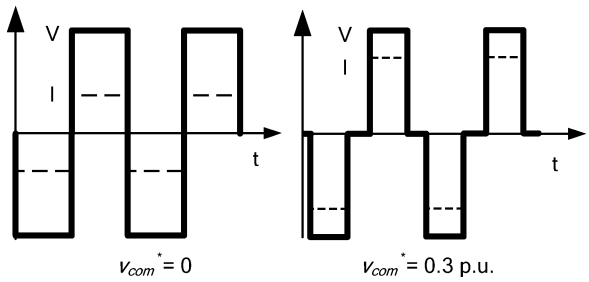

Fig. 8. Current and voltage wave pattern according to the difference in the common mode duty ratio at constant power.

C. Design of the Transformer

The major focus in the design for the transformer is the current capacity. This is because the transformer has two functions: dc active filter and isolation transformer. The transformer current $I_{\rm tran}$ is equaled to the sum of the active filter current $I_{\rm com}$ and the current $I_{\rm dif}$, according to the output power shown in

$$I_{\rm trans} = I_{\rm dif} + \frac{I_{\rm com}}{2}. \tag{6}$$

Note that in (6), the active filter current is divided by 2, because the transformer winding is connected in parallel to the center tap in the common-mode circuit, as shown in Fig. 4(c) and (d).

The common-mode voltage controls the capacitor voltage variation, and the differential-mode voltage controls the transmission power to the power grid. The common-mode voltage should be varied widely to suppress the capacitance, as shown in (5). However, the output period of the common-mode voltage is limited by the output period of the differential mode, i.e., the duty ratio $D_{\rm dif}$ for the differential mode can be constrained by

$$D_{\rm dif} + D_{\rm com} = 1 \tag{7}$$

where $D_{\rm com}$ is the duty ratio for the common-mode voltage.

Fig. 8 shows the differential-mode current waveforms and the terminal voltage waveforms of the transformer when the common-mode command is 0 and 0.3 p.u., given at the same output power. The differential-mode current increases when the common-mode voltage increases, because the power transmission period is reduced by the common-mode voltage. Therefore, a large common mode voltage causes a large current in the transformer. The transformer current is then obtained as the next step.

The duty ratio for the common-mode voltage is obtained by (8), because the average voltage V_{cf0} of the capacitor C_f is half of the dc voltage used to achieve the maximum capacitor voltage variation

$$D_{\rm com} = \frac{\Delta V_{cf}}{2V_{cf0}} = \frac{\Delta V_{cf}}{V_{\rm dc}} \tag{8}$$

where $V_{\rm dc}$ is the dc voltage of the first-stage inverter.

The differential-mode current $I_{\rm dif}$ is then obtained using (9) from (7) and (8) as

$$I_{\rm dif} = \frac{P_{\rm in}}{V_{\rm dc} D_{\rm dif\_max}} = \frac{P_{\rm in}}{V_{\rm dc} - \Delta V_{cf}}. \tag{9}$$

On the other hand, the common-mode current $I_{\rm com}$ is defined by (10), because the maximum value of the power ripple is twice that of the input power

$$I_{\rm com} = \frac{2P_{\rm in}}{V_{\rm dc}}. \tag{10}$$

Finally, the transformer current $I_{\rm trans}$ is obtained by (11) from (6), (9), and (10) as

$$I_{\rm trans} = I_{\rm dif} + \frac{I_{\rm com}}{2} = \frac{P_{\rm in}}{V_{\rm dc} - \Delta V_{cf}} + \frac{P_{\rm in}}{V_{\rm dc}}. \tag{11}$$

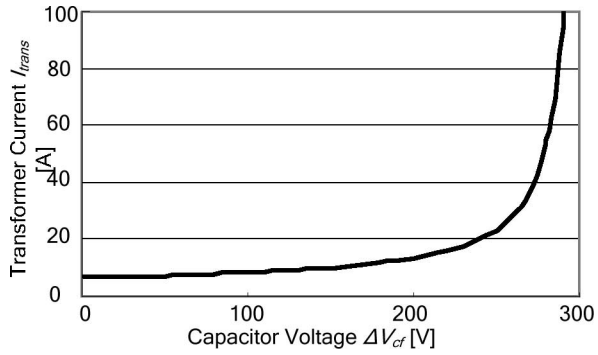

Fig. 9. Current capacity of the transformer necessary for compensation ($P_{\rm in} = 1$ kW, $V_{\rm dc} = 300$ V, $V_{cf0} = 150$ V).

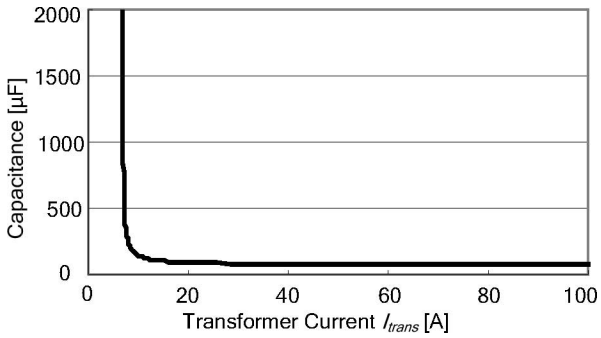

Fig. 10. Current capacity and capacitance of the transformer necessary for compensation ($P_{\rm in} = 1$ kW, $V_{\rm dc} = 300$ V, $V_{cf0} = 150$ V, 1000 μF = 3.18 p.u).

It should be noted that $I_{\rm com}$ in (10) is the peak value of the common-mode current. Therefore, the rms value $I_{\rm trans(rms)}$ of the transformer current, which is used to determine the thickness of the transformer winding, is obtained by

$$I_{\rm trans(rms)} = I_{\rm dif} + \frac{I_{\rm com}}{2} = \frac{P_{\rm in}}{V_{\rm dc} - \Delta V_{c_f}} + \frac{P_{\rm in}}{\sqrt{2}V_{\rm dc}}. \quad (12)$$

Fig. 9 presents the relation between the transformer current and the capacitor voltage variation at $V_{cf0} = 150$ V, $P_{\rm in} = 1$ kW, and $V_{\rm dc} = 300$ V. As the capacitor voltage variation increases, a smaller active filter capacitor C_f can be achieved. However, as the capacitor voltage variation becomes larger, it results in a system that requires a large current capacity transformer. It should be noted that the current rating of the switching device is also dominated by (11).

In addition, the relation between the transformer current and the capacitance is represented by (13), from (5) and (11), as

$$C_f = \frac{P_{\rm in}(P_{\rm in} - V_{\rm dc} I_{\rm trans})}{\omega V_{c_{f0}} V_{\rm dc}(2P_{\rm in} - V_{\rm dc} I_{\rm trans})}. \quad (13)$$

Fig. 10 further illustrates the relation between the transformer current and the capacitance for $V_{cf0} = 150$ V, $P_{\rm in} = 1$ kW, and $V_{\rm dc} = 300$ V. Fig. 10 shows that selection of a smaller capacitance results in the requirement of a larger current capacity transformer. For example, if a 150-μF capacitor is selected for a 1-kW system, then a transformer with a current capacity of more than 10 A must be considered. In other words, the proposed method requires a fat winding transformer compared with that required for the conventional circuit.

TABLE II
EXPERIMENTAL PARAMETERS WITH PERCENTAGE IMPEDANCE SHOWN IN PARENTHESES

Output power	1 [kW]
Grid frequency	50 [Hz]
Grid voltage	200 [V]
AC Link frequency	10 [kHz]
Active filter inductor	5 [mH] (4%)
Energy buffer capacitor	440 [μF] (18%)
DC link capacitor (Proposed circuit)	110 [μF] (72%)
DC link capacitor (Conventional circuit)	2200 [μF] (3.6%)

Note that the number of turns in the transformer winding is calculated from (14), as for the conventional transformer

$$N = \frac{V_{\rm dc}}{4fSB} \quad (14)$$

where N is the number of turns in the winding, f is the switching frequency of the first-stage inverter, B is the flux density of the core, and S is the section area of the core.

IV. EXPERIMENTAL RESULTS

The proposed converter was tested to confirm the validity of the proposed circuit operation using the experimental conditions given in Table II. The proposed control shown in Fig. 6 is implemented using a digital control system with a digital signal processor (DSP). The auxiliary inductor is connected to the center tap of the transformer, because the leakage inductance of the transformer is not sufficient to reduce the switching ripple current.

Fig. 11 shows the operation waveforms of the conventional circuit without a dc active filter. A sinusoidal grid current waveform and unity power factor are obtained; however, the dc input current has a large ripple current component of 100 Hz.

Fig. 12 shows the operation waveforms of the proposed converter. The ripple of the dc input current is suppressed to 20% that of the conventional circuit, which indicates that the dc active filter function is effective. The grid current waveform maintains the sinusoidal waveform and unity power factor.

Fig. 13 shows the operation waveforms of the conventional circuit using a large electrolytic capacitor of 2200 μF. This circuit was tested in order to determine the reduction in the dc ripple current using a large electrolytic capacitor. Although the

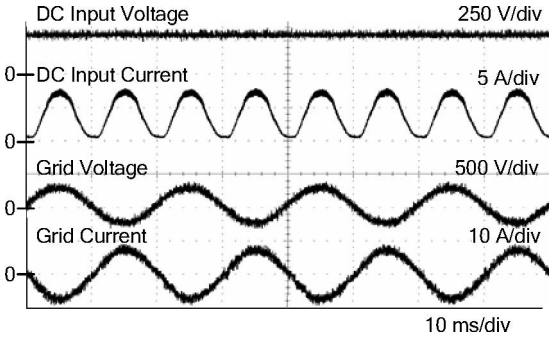

Fig. 11. Operation waveforms of the conventional circuit without a dc active filter.

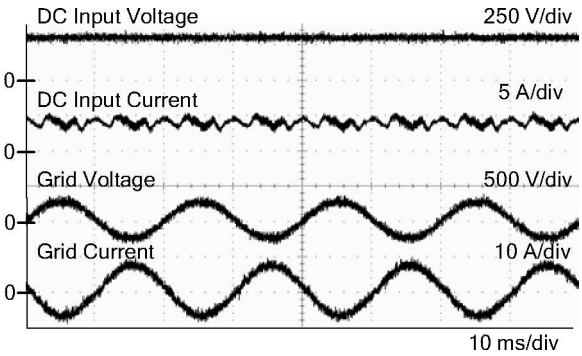

Fig. 12. Operation waveforms of the proposed circuit.

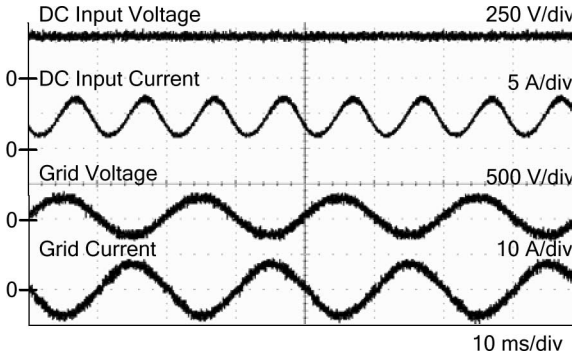

Fig. 13. Operation waveforms of the conventional circuit with a large electrolytic capacitor $C_{\mathrm{dc2}} = 2200\ \mu$F.

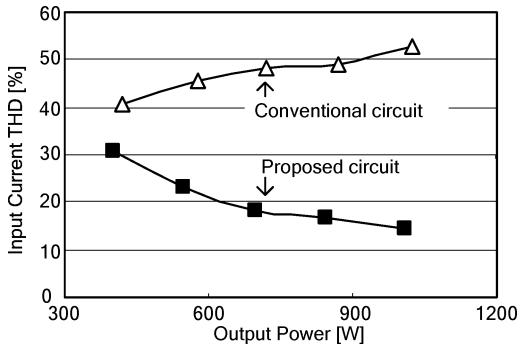

Fig. 14. Input dc current distortion factor.

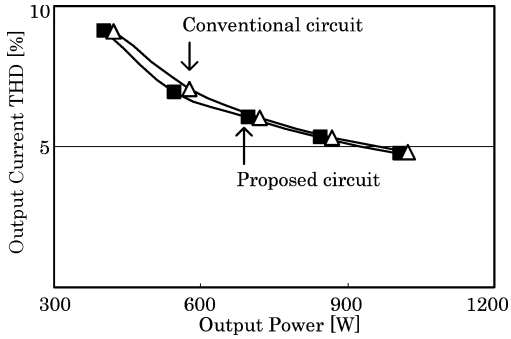

Fig. 15. THD of the grid connection current for the conventional and proposed circuits.

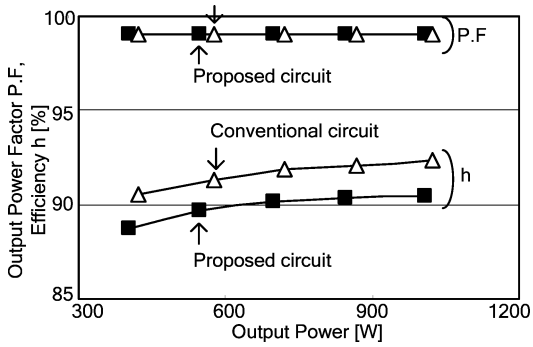

Fig. 16. Efficiency and grid connection power factor.

large electrolytic capacitor used is 20 times than that shown in Fig. 12, the dc input current was not significantly reduced.

Fig. 14 shows the dc input current total harmonic distortion (THD) of the conventional and proposed circuit, which is defined by (14)

$$I_{\mathrm{dc\_THD}} = \frac{\sqrt{\sum I_n^2}}{I_{\mathrm{dc}}} \tag{15}$$

where I_n is the harmonic components and I_{dc} is the dc component.

The major harmonic component in the input current is 100 Hz. In a conventional circuit, the dc input current THD increases according to the increment of the output power. In contrast, the dc input current THD decreases despite the increment of the output power in the proposed circuit, i.e., the proposed circuit is suitable for high-power applications, due to its effectiveness in the high-output power region.

Fig. 15 shows the THD of the grid interconnection current for the conventional and proposed circuits; almost the same current THD values were obtained. Therefore, the proposed circuit can achieve the same performance level as the conventional circuit.

Fig. 16 shows the efficiency and the grid interconnection power factor of the conventional and proposed circuits. The efficiency of the conventional circuit is higher than the proposed circuit. One of the reasons for the increase in power loss is the increasing current in the transformer. Therefore, the efficiency of the proposed circuit can be improved if the design of the transformer is optimized. Note that the proposed converter has good performance as a grid interconnection converter, because both power factors of the proposed circuit and the conventional circuit are 99%.

The experimental results confirm that the proposed converter is valid for the reduction of the dc input ripple current in a dc power supply, without the need for large electrolytic capacitors.

V. Conclusion

A novel single-phase isolated converter was proposed for grid interconnection applications. The ripple current in a dc power supply, such as a fuel cell, battery, or photovoltaic cell, can be reduced by the appropriate operation of a dc active filter. The main feature of the proposed circuit is that it does not require additional switching devices, because the zero vector of the first-stage inverter is controlled as the dc active filter. A 1-kW prototype was constructed based on the proposed circuit, and the following experimental results were obtained.

1) The ripple current can be decreased to 20% that of the conventional circuit.
2) The proposed circuit shows a degree of effectiveness for high output power applications.
3) The total electrolytic capacitor requirement of the system is decreased to 25% that of the conventional circuit.
4) The dc active filter operation in the proposed method circuit does not interfere with the grid interconnection current control.

In future work, optimization of the transformer and construction of a high-power prototype will be undertaken.

References

[1] S. Sumiyoshi, H. Omuri, and Y. Nishida, "Power conditioner consisting of utility interactive inverter and soft-switching DC–DC converter for fuel-cell cogeneration system," in *Proc. IEEE PCC 2007*, Nagoya, Japan, pp. 455–462.

[2] R. Nojima, I. Takano, and Y. Sawada, "Transient performance of a new-type hybrid electric power distributed system with fuel cell and SMES," in *Proc. IEEE IECON 2001*, pp. 1303–1308.

[3] H. Cha, J. Choi, and B. Han, "A new three-phase interleaved isolated boost converter with active clamp for fuel cells," in *Proc. IEEE PESC 2008*, pp. 1271–1276.

[4] L. Danwei and L. Hui, "A three-port three-phase DC–DC converter for hybrid low voltage fuel cell and ultracapacitor," in *Proc. IEEE IECON 2006*, pp. 2258–2563.

[5] P. T. Krein and R. Balog, "Low cost inverter suitable for medium-power fuel cell sources," in *Proc. IEEE PESC 2002*, pp. 321–326.

[6] B. Bouneb, D. M. Grant, A. Cruden, and J. R. McDonald, "Grid connected inverter suitable for economic residential fuel cell operation," in *Proc. IEEE EPE 2005*, p. 10.

[7] S. Jung, Y. Bae, S. Choi, and H. Kim, "A low cost utility interactive inverter for residential fuel cell generation," *IEEE Trans. Power Electron.*, vol. 22, no. 6, pp. 2293–2298, Nov. 2007.

[8] J.-M. Kwon and B.-H. Kwon, "High step-up active-clamp converter with input-current doubler and output-voltage doubler for fuel cell power systems," *IEEE Trans. Power Electron.*, vol. 24, no. 1, pp. 108–115, Jan. 2009.

[9] D. Polenov, H. Mehlich, and J. Lutz, "Requirements for MOSFETs in fuel cell power conditioning applications," in *Proc. IEEE EPE-PEMC 2006*, pp. 1974–1979.

[10] G. Fontes, C. Turpin, S. Astier, and T. A. Meynard, "Interactions between fuel cells and power converters: Influence of current harmonics on a fuel cell stack," *IEEE Trans. Power Electron.*, vol. 22, no. 2, pp. 670–678, Mar. 2007.

[11] C. Liu and J.-S. Lai, "Low frequency current ripple reduction technique with active control in a fuel cell power system with inverter load," *IEEE Trans. Power Electron.*, vol. 22, no. 4, pp. 1429–1436, Jul. 2007.

[12] S. K. Mazumder, R. K. Burra, and K. Acharya, "A ripple-mitigating and energy-efficient fuel cell power-conditioning system," *IEEE Trans. Power Electron.*, vol. 22, no. 4, pp. 1437–1452, Jul. 2007.

[13] F. Perfumo, A. Tenconi, M. Cerchio, R. Bojoi, and G. Gianolio, "Fuel cell for electric power generation: Peculiarities and dedicated solutions for power electronic conditioning systems," *EPE J.*, vol. 16, pp. 44–50, Feb. 2006.

[14] M. Pereira, G. Wild, H. Huang, and K. Sadek, "Active filters in HVDC systems: Actual concepts and application experience," in *Proc. Int. Conf. Power Syst. Technol. 2002. (PowerCon)*, pp. 989–993.

[15] M. Saito and N. Matsui, "Modeling and control strategy for a single-phase PWM rectifier using a single-phase instantaneous active/reactive power theory," in *Proc. IEEE INTELEC 2003*, pp. 573–578.

[16] X. Ma, B. Wang, F. Zhao, G. Qu, D. Gao, and Z Zhou, "A high power low ripple high dynamic performance DC power supply based on thyristor converter and active filter," in *Proc. IEEE IECON 2002*, pp. 1238–1242.

Jun-ichi Itoh (A'04–M'04) was born in Tokyo, Japan, in 1972. He received the M.S. and Ph.D. degrees in electrical and electronic systems engineering from Nagaoka University of Technology, Nagaoka, Japan, in 1996 and 2000, respectively.

Form 1996 to 2004, he was with Fuji Electric Corporate Research and Development, Ltd., Tokyo, Japan. Since 2004, he has been an Associate Professor in Nagaoka University of Technology, Niigata, Japan. His current research interests include matrix converters, dc/dc converters, power factor correction techniques, and motor drives.

Dr. Itoh is a member of the Institute of Electrical Engineers of Japan. He received the Institute of Electrical Engineers of Japan (IEEJ) Academic Promotion Award (IEEJ Technical Development Award) in 2007.

Fumihiro Hayashi was born in Kagawa, Japan, in 1985. He received the B.S. and M.S. degrees in electrical, electronics and information engineering from Nagaoka University of Technology, Niigata, Japan, in 2007 and 2009, respectively.

Since 2009, he has been with Shikoku Electric Power Company, Inc., Kagawa, Japan. His current research interests include power grid distribution systems and new converter topologies.